Behavior of Electron Density Functions in Molecular Interactions

John Bentley†

Radiation Laboratory, University of Notre Dame, Notre Dame, Indiana 46556-0579

Received: April 7, 1998; In Final Form: May 15, 1998

When molecules approach each other at distances typical of gas-phase complexes or condensed-phase media, it is known that the intermolecular electron density function in the region between the molecules is related to the strength of the intermolecular interaction. We explore this behavior for 50 interaction pairs, and find that, in the interaction region, the total electron density is well represented by the sum of the density functions of the isolated molecules. The minimum in the electron density function between pairs of interacting molecules is used to estimate the sizes of the molecules. Taken in conjunction with the density additivity in this region, this procedure provides a means of estimating molecular sizes without performing supermolecule calculations. For weakly interacting systems, the distances and density minima identified by this procedure are consistent with use of the 0.002 au isodensity surface to define the size and shape of a molecule in condensed media.

Introduction

The molecular electron density function, defined by eq 1,

$$\rho(\boldsymbol{r}_1) = N \int ... \int |\Psi(\chi_1,\chi_2,...\chi_N)|^2 d\sigma_1 d\chi_2 d\chi_3 ... d\chi_N,\ \chi = \{\boldsymbol{r}, \sigma\} \quad (1)$$

contains a wealth of information about the isolated molecule.[1] Many electrostatic molecular properties, such as dipole moments and electrostatic potentials, can be directly determined from the density function. Because X-rays scatter from electrons, the density function can, in principle, be extracted from crystal X-ray diffraction data.[2] In 1967, Bader, Henneker, and Cade[3] suggested that the surface generated by an electron isodensity contour provided a useful theoretical definition of the size and shape of an isolated molecule. They specifically proposed the 0.002 au density contour but pointed out that other choices were also reasonable. (1 au of electron density = 1 electron per bohr^3; 1 bohr = 0.0529177 nm.)

Interest has been shown in using molecular electron density to define molecular size and shape in condensed media,[4−7] but rationalization of this concept is not without difficulties. At the nearest-neighbor distances characteristic of liquids or solids, molecules interact with their neighbors and are subject to various external forces, such as polarization, induction, dispersion, overlap repulsion, and hydrogen bonding, which will perturb the electron density from its gas-phase distribution. However, if a molecule retains its identity in going from gaseous to condensed phase, the size and shape indicated by the gas-phase electron density may be expected to be reliable indicators of those properties in the liquid or solid. The results discussed next bear out this expectation.

In the present work, we look to the density functions themselves to provide some guidance concerning molecular boundaries. We will use the properties of the electron density functions of systems of interacting molecules to define the sizes and shapes of molecules in condensed media. To represent the nearness of neighbors characteristic of the condensed environment, we take pairs of molecules at distances and configurations reported from experimental studies such as liquid or crystal diffraction, crossed-beam scattering, or spectroscopy of van der Waals molecules. Some theoretically determined minimum-energy structures are also included; in several cases, theoretical potential surfaces have been used jointly with experiment to arrive at more detailed characterizations of the interactions. In this work we take the supermolecular structure as specified by the literature, compute the supermolecular electron density function, and examine various properties of that density function. In all cases examined here, the interacting molecules are closed-shell species, and the models presented are specific to closed-shell interactions.

At the nearest-neighbor distances characteristic of liquids and solids, molecular electron clouds significantly interpenetrate each other. However, if we define the boundary of the molecule by the minimum in the total electron density as we pass from one molecule to another, we have a prescription for molecular size in which mutual penetration is minimal. This concept is not new. In an early application of it, Gourary and Adrian[8] used the minima in experimental electron densities for alkali halide crystals to define revised ionic radii for alkali cations and halide anions. This concept is also central in the extension to intermolecular interactions of Bader's theory of atoms in molecules.[1]

The contributions of Bader on the topic of the electron density function have been so extensive that many of the observations made herein are dealt with in ref 1, and it is fair to ask what is new here. The answer is that by examining the density function in *less* detail than Bader and his colleagues do, we are able to obtain a simplified description of the density function in the region between interacting molecules. We observe that the total electron density of the supermolecular complex *in the region of interaction* is well represented by the sum of the densities of the isolated molecules. This additivity of electron densities is a very useful finding, in that it may permit us to draw certain conclusions about molecules in condensed environments without conducting detailed calculations of the environments. We identify a specific molecular isodensity contour that is descriptive in an average sense of the size and shape of a molecule in a condensed medium.

† E-mail: bentley.1@nd.edu.

S1089-5639(98)01760-5 CCC: $15.00
Published on Web 06/29/1998

TABLE 1: Compilation of r_m and $\rho(r_m)$ for Supermolecules AB Using Known Geometries and Comparison with Additivity Model

A	B	geometry	r_m, Å[a]	$\rho(r_m)$, au	r_m^{fit}, Å[a]	$\rho^{fit}(r_m)$, au	source of geometry[b]
He	He	$\boldsymbol{R} = 2.97$ Å	1.485	0.00090	1.485	0.00087	MB[14]
	Ne	$\boldsymbol{R} = 3.005$ Å	1.380	0.00147	1.389	0.00141	GTC[15]
	Ar	$\boldsymbol{R} = 3.434$ Å	1.448	0.00149	1.411	0.00150	GTC[15]
	Na^+	$\boldsymbol{R} = 2.43$ Å	1.21	0.00430	1.19	0.00386	QC consistent with GTC[16]
	F^-	$\boldsymbol{R} = 3.52$ Å	1.52	0.00108	1.48	0.00108	QC[17]
	CO_2	$\boldsymbol{R} = 3.15$ Å, C_{2v} structure	1.39	0.00169	1.38	0.00170	MB[18]
	CH_4	$\boldsymbol{R} = 3.4$ Å, C_{3v} face structure	1.44	0.00144	1.43	0.00141	QC[19]
Ne	Ne	$\boldsymbol{R} = 3.10$ Å	1.55	0.00214	1.55	0.00199	MB[20]
	Ar	$\boldsymbol{R} = 3.516$ Å	1.591	0.00203	1.577	0.00206	GTC[15]
	F^-	$\boldsymbol{R} = 3.23$ Å	1.50	0.00337	1.50	0.00343	QC[21]
	Cl^-	$\boldsymbol{R} = 3.89$ Å	1.64	0.00175	1.63	0.00185	QC[21]
	HF	$\boldsymbol{R}_{NeF} = 3.40$ Å, Ne−H−F, linear	1.52	0.00328	1.50	0.00313	QC consistent with IR[12]
		$\boldsymbol{R}_{NeF} = 3.07$ Å, Ne−F−H, linear	1.52	0.00265	1.52	0.00249	
	CH_4	$\boldsymbol{R} = 3.5$ Å, C_{3v} face structure	1.62	0.00182	1.61	0.00181	QC[19]
Ar	Ar	$\boldsymbol{R} = 3.76$ Å	1.88	0.00290	1.88	0.00311	UV/vis[22]
	F^-	$\boldsymbol{R} = 3.09$ Å	1.61	0.00887	1.61	0.0103	QC[21]
	Cl^-	$\boldsymbol{R} = 3.73$ Å	1.79	0.00467	1.79	0.00548	QC[21]
	HF	$\langle \boldsymbol{R}_{ArF} \rangle_{vib} = 3.54$ Å, $\theta_{ArFH} = 48.2°$	1.85	0.00318	1.85	0.00317	MW[23]
		$\boldsymbol{R}_{ArF} = 3.51$ Å, Ar−H−F, linear	1.72	0.00616	1.71	0.00607	MW, far IR and IR[24]
		$\boldsymbol{R}_{ArF} = 3.29$ Å, Ar−F−H, linear	1.79	0.00381	1.79	0.00398	
	H_2O	$\boldsymbol{R}_{OAr} = 3.65$, $\theta_{HOAr} = 19°$, planar	1.77	0.00478	1.77	0.00461	IR[25]
	CO_2	$\boldsymbol{R} = 3.49$ Å, planar, C_{2v}	1.85	0.00330	1.85	0.00341	MW[26]
	CH_4	$\mathbf{R} = 3.55$ Å, face approach	1.83	0.00378	1.83	0.00406	MB[27]
		$\boldsymbol{R} = 4.00$ Å, along CH bond	1.77	0.00483	1.77	0.00500	
	C_2H_4	$\boldsymbol{R} = 3.6$ Å, planar, C_{2v}	1.85	0.00365	1.86	0.00382	IR[28]
H_2O	H_2O	$\boldsymbol{R}_{OO} = 2.98$ Å, $\theta_{acceptor} = 58.5°$, $\theta_{donor} = -50.2°$	1.32[c]	0.0196	1.32[c]	0.0213	ER[29]
		$\boldsymbol{R}_{OO} = 2.85$ Å, tetrahedral hydrogen-bonded structure	1.29[c]	0.0323	1.29[c]	0.0349	LXD[30]
	Cl^-	$\boldsymbol{R}_{OCl} = 3.178$ Å, hydrogen bond geometry	1.653	0.0222	1.706	0.0209	LXD/LND[31]
	NH_4^+	$\boldsymbol{R}_{NO} = 3.08$ Å, NH−O hydrogen bond	1.35	0.0200	1.38	0.0233	LXD[32]
	Li^+	$\boldsymbol{R}_{LiO} = 2.25$ Å, nonplanar	1.43	0.0139	1.44	0.0143	LXD/LND[31]
		$\boldsymbol{R}_{LiO} = 1.858$ Å, C_{2v}	1.16	0.0336	1.14	0.0314	QC[33]
	Na^+	$\boldsymbol{R}_{NaO} = 2.44$ Å, nonplanar	1.36	0.0161	1.39	0.0194	LXD[11]
	HF	$\boldsymbol{R} = 2.64$ Å, C_{2v} structure	1.17	0.0342	1.19	0.0325	QC[34]
	CH_4	$\boldsymbol{R}_{CO} = 3.70$ Å, O−HC	1.58	0.00740	1.61	0.00953	IR[35]
		$\boldsymbol{R}_{CO} = 3.70$ Å, OH−C	2.00	0.00438	2.01	0.00427	
	CO_2	$\boldsymbol{R}_{CO} = 2.79$ Å, planar nonhydrogen-bonded structure	1.43	0.0106	1.43	0.0117	IR[36]
CH_4	CH_4	$\boldsymbol{R}_{CC} = 4.0$ Å, C_{3v} interaction	2.29[d]	0.00407	2.29[d]	0.00416	LXD[37]
C_2H_4	C_2H_4	$\boldsymbol{R} = 4.067$ Å between molecular centers, C=C bonds parallel and tilted 14.6° from $\boldsymbol{R}$	1.973[e]	0.00283	1.973[e]	0.00293	CXD[38]
	HF	$\boldsymbol{R} = 3.3$ Å, C_{2v} nonplanar	1.57	0.0104	1.57	0.00997	QC[34]
CO_2	CO_2	$\boldsymbol{R}_{CC} = 3.47$ Å, OCC angle = 55°, parallel shifted	1.43[f]	0.0101	1.43[f]	0.0106	electric deflection[39] and QC[40]
HF	HF	$\boldsymbol{R}_{FF} = 2.75$ Å, hydrogen-bonded nonlinear	1.55[g]	0.0201	1.53[g]	0.0205	QC[41]
Li^+	F^-	$\boldsymbol{R} = 2.0132$ Å	0.758	0.0245	0.781	0.0195	CXD[42]
		$\boldsymbol{R} = 1.5639$ Å	0.608	0.0723	0.652	0.0657	UV/vis[43]
	Cl^-	$\boldsymbol{R} = 2.5699$ Å	0.845	0.0152	0.883	0.00896	CXD[42]
		$\boldsymbol{R} = 2.0207$ Å	0.687	0.0448	0.751	0.0310	UV/vis[43]
	HF	$\boldsymbol{R}_{LiF} = 1.793$ Å, linear	0.709	0.0295	0.717	0.0278	QC[33]
	C_2H_4	$\boldsymbol{R} = 2.358$ Å, C_{2v} nonplanar	0.837	0.0155	0.862	0.0102	QC[33]
Na^+	F^-	$\boldsymbol{R} = 2.3171$ Å	1.041	0.0209	1.063	0.0191	CXD[42]
		$\boldsymbol{R} = 1.9620$ Å	0.914	0.0459	0.944	0.0469	UV/vis[43]
	Cl^-	$\boldsymbol{R} = 2.8201$ Å	1.130	0.0138	1.165	0.0104	CXD[42]
		$\boldsymbol{R} = 2.3609$ Å	0.975	0.0338	1.036	0.0278	UV/vis[43]

[a] The parameter r_m is reckoned from the heavy nucleus in molecule A; use $\boldsymbol{R} - r_m$ to obtain the minimum distance relative to molecule B. [b] The following abbreviations are used for sources of geometries: MB, crossed molecular beam; GTC, gas transfer coefficients; QC, quantum chemical results; IR, infrared spectroscopy; MW, microwave spectroscopy; ER, electric resonance spectroscopy; LXD, X-ray diffraction of liquids; LND, neutron diffraction of liquids; CXD, X-ray diffraction of crystals; UV/vis, optical spectroscopy of gaseous molecules. [c] Distance from proton-accepting oxygen. [d] Distance from proton-donating carbon. [e] Distance from carbon to nearest carbon on other monomer ($\boldsymbol{R}_{CC} = 3.946$ Å). [f] Distance from oxygen in direction of nearest oxygen on other molecule ($\boldsymbol{R}_{OO} = 2.86$ Å). [g] Distance from proton-donating fluorine.

In the next section, the procedures for obtaining, describing, and probing electron densities will be discussed. The following section presents results for ~50 specific molecular interactions. Finally, conclusions will be presented.

Procedure

This work requires knowledge of the electron density functions of isolated molecules A and B and of the supermolecule AB formed by bringing them together. There are five density functions of interest: $\rho_A(\boldsymbol{r})$, $\rho_B(\boldsymbol{r})$, $\rho_{AB}(\boldsymbol{r};\boldsymbol{R})$, $\rho_{AB}{}^0(\boldsymbol{r};\boldsymbol{R})$, and the difference function

$$\Delta\rho_{AB}(\boldsymbol{r};\boldsymbol{R}) = \rho_{AB}(\boldsymbol{r};\boldsymbol{R}) - \rho_A(\boldsymbol{r}) - \rho_B(\boldsymbol{r}) = \rho_{AB}(\boldsymbol{r};\boldsymbol{R}) - \rho_{AB}{}^0(\boldsymbol{r};\boldsymbol{R}) \quad (2)$$

in which $\boldsymbol{R}$ is a suitably defined vector from A to B with length R, $\rho_{AB}{}^0(\boldsymbol{r};\boldsymbol{R})$ is the sum of isolated-molecule density functions, and the origin of the electronic coordinate $\boldsymbol{r}$ is at the origin of molecule A. The relative positions of molecules A and B and the distance $\boldsymbol{R}$ are taken from the literature as described in Table

1. (In studies of intermolecular potential energy surfaces, orientation angles Ω_A and Ω_B are necessary to completely describe the complex. The present work deals with complexes at a few specified geometries, and the orientation variables will be left implicit to simplify notation.) The density functions for all systems are determined by ab initio calculations[9] at the MP2/6-311+G** level, with molecular geometries optimized at the RHF/6-311G** level. The molecular geometries within the supermolecule are frozen at isolated-molecule values. All computed densities are the relaxed MP2 densities recommended by Wiberg et al.[10] (i.e., they are computed by energy derivative rather than expectation value methods). Density functions discussed later have been computed on a fine mesh and interpolated as necessary.

Many of the calculations discussed here were also conducted with 6-311G** basis sets and/or at the RHF level. It was found that the presence of diffuse functions ("+") made a small but nonnegligible difference for anions and polar molecules with lone pairs. The differences between RHF and MP2 were slight and had no effect on the conclusions.

Several properties of $\rho_{AB}(\boldsymbol{r};\boldsymbol{R})$ and $\rho_{AB}{}^0(\boldsymbol{r};\boldsymbol{R})$ are useful for characterizing the interaction: r_m is the position along $\boldsymbol{R}$ of the minimum of $\rho_{AB}(\boldsymbol{r};\boldsymbol{R})$, $\rho_{AB}(r_m;\boldsymbol{R})$ is the value of the density at the minimum, and r_m lies very close to the (3,−1) intermolecular bond critical point discussed by Bader.[1] Indeed, if $\boldsymbol{R}$ coincides with a symmetry element, they are generally identical. In Bader's theory of atoms in molecules, the boundary between an atom and its neighbors is defined by a surface of zero flux in the gradient of the electron density function, and the bond critical point is the saddle point along a line that joins nucleus A to nucleus B. The value of the density function at the bond critical point is diagnostic of the strength of the bond. The interested reader should consult Bader's monograph for details of this theory. The parameter r_m differs from the critical point in that the latter is the origin of two trajectories of $\nabla\rho(\boldsymbol{r})$ that terminate at nuclei A and B, whereas the former is the minimum density point along the straight line $\boldsymbol{R}$ joining A and B. Our concern here is that the zero flux surface can define the boundary between two interacting molecules. The term r_m, which lies on this surface at or near the critical point, is indicative of the size of a molecule in a populated environment, and $\rho(r_m)$ is indicative of the strength of its interaction with that environment.

It is also useful to define the same properties for the noninteracting density $\rho_{AB}{}^0(\boldsymbol{r};\boldsymbol{R})$. The terms $r_m{}^0$ and $\rho_{AB}{}^0(r_m{}^0)$ can be compared with the corresponding properties of the supermolecular density. The extent to which they differ quantifies the ability of $\rho_{AB}{}^0$ to describe molecular interactions.

As defined in eq 2, $\Delta\rho_{AB}$ is a measure of the distortion each molecule undergoes as a result of its interaction with the other participant in the supermolecule. For the systems discussed later, which involve neither chemical reaction nor significant charge transfer, $\Delta\rho_{AB}$ vanishes smoothly as the intermolecular distance $\boldsymbol{R}$ increases. A study of the global properties of $\Delta\rho_{AB}$ would be interesting in its own right, but this work concentrates on $\Delta\rho_{AB}$ in the region of the intermolecular contact, specifically, along the line defined by the vector $\boldsymbol{R}$.

Features of Intermolecular Charge Densities

We first make an examination of an interacting system characterized by strong intermolecular attraction and one with weaker attraction. Our purpose is to identify the limits of usefulness of isolated-molecule density functions in characterizing molecular interactions. The strongly bound system is the sodium ion−water complex, the other the neon−hydrogen fluoride van der Waals molecule. Planar sections of the supermolecular densities and corresponding difference densities are shown in Figures1 and 2.

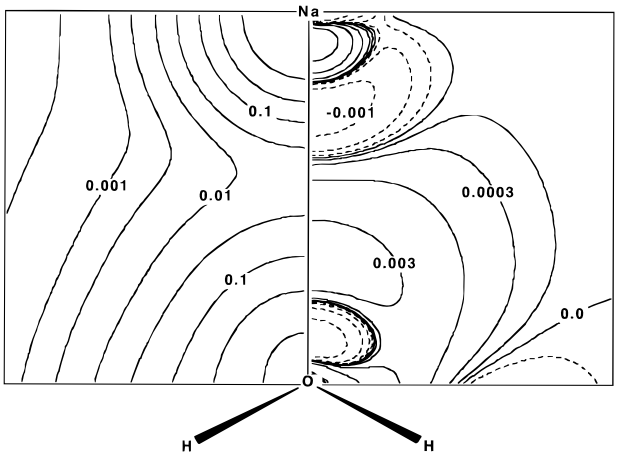

Figure 1. Supermolecular MP2 electron density (left side) and difference density (right side) for the complex $Na^+—OH_2$, at a Na—O distance of 2.44 Å. The plane shown contains the Na and O nuclei. The plane containing the H and O nuclei makes an angle of 135° with the plane of the figure. The contours, in au, are in logarithmic steps of 1.0, 0.3, 0.1, 0.03, etc. Negative contours are displayed with dashed lines.

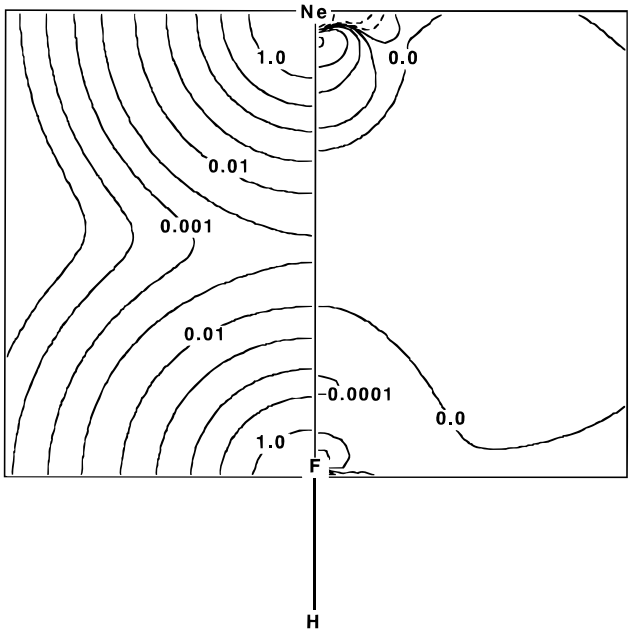

Figure 2. Supermolecular MP2 electron density (left side) and difference density (right side) for the linear complex Ne—FH, at a Ne—F distance of 3.07 Å. The contours, in au, are in logarithmic steps of 1.0, 0.3, 0.1, 0.03, etc. Negative contours are displayed with dashed lines.

The sodium cation−water molecule complex is displayed in Figure 1, in a plane that contains the Na—O bond. The ion is located out of the plane of the water molecule, at a distance of 2.44 Å, as indicated by X-ray diffraction data[11] of aqueous solutions of $NaNO_3$. The angle between the Na—O vector and the HOH bisector is 135°. The supermolecular density was computed from a MP2/6-311+G** density function. The difference density $\Delta\rho_{AB}$ was determined by subtracting the Na^+ and H_2O MP2 density functions from that of the complex. In the plane depicted, the supermolecular density has a saddle point between Na and O, at which the density is 0.0161 au. At the same point, the difference density is 0.0009 au. This is a typical

feature of such maps: The difference density is an order of magnitude smaller than the supermolecular density in that part of space where both molecules make significant contributions. Sizable density distortions are evident in Figure 1, but they occur within 1 Å of the nuclei, which is outside the range of significant penetration of density from the other member of the complex. In the vicinity of r_m, the sum of isolated-molecule densities gives a quite satisfactory representation of the supermolecular density. Even in a strongly interacting complex such as $Na^+—OH_2$, the deformation density is only a minor contribution.

The second thing to note about the difference density is that its variation as one moves perpendicularly away from the Na—O vector is much less than its variation along that vector. The planar slice gives more data but not more information. This result suggests that the behavior of density functions along a single line passing through the zone of greatest intermolecular interaction can characterize the interaction. (Of course, interactions involving a concave region of a molecule would need more information than provided by a single line.)

The same features can be seen in Figure 2, where density functions for neon atom aligned linearly with the fluorine end of a rigid hydrogen fluoride molecule are shown. In this case the geometry of the van der Waals complex was taken from a quantum chemical potential surface[12] that was able to reproduce the infrared spectrum of the complex. The density at r_m is 0.00265 au and the difference density is −0.000011 au. In this system, the isolated-molecule densities are an excellent approximation to the supermolecular density.

The difference densities for the two systems just discussed were also computed after applying a counterpoise correction;[13] that is, the isolated molecule density functions were determined using the supermolecule basis sets and subtracted from the supermolecule density functions. The corrected difference densities (not shown) varied slightly from the uncorrected densities, but exhibited the same general shapes and small values in the regions of the minima. We conclude that application of the counterpoise correction provides no additional insight to this work.

With these general findings in hand, we will examine a large assortment of intermolecular interactions on the basis of the density along a line joining their nearest neighboring atoms.

Results

There is a wealth of experimental and theoretical information in the literature on intermolecular interactions, separations, and orientations. By assembling supermolecules from isolated molecules according to structures reported in these sources, we seek to establish regularities in the electron density in the interaction region. In Table 1 we collect data for ∼50 systems for which intermolecular interaction data appear in the literature. The supermolecular structures from these reports are analyzed to provide positions of minima r_m and corresponding minimum electron densities $\rho(r_m)$ for the systems described.

The interactions characterized in Table 1 are drawn from a variety of sources. Most of the spectroscopic and theoretical results pertain to gas-phase van der Waals or hydrogen-bound complexes between two molecules. The diffraction results refer to a molecule interacting with a large number of neighbors. The interaction data assembled here are not uniform in quality or degree of specificity, nor is it necessary that they be so. Their important feature is that they span a range of types and environments of molecular interaction, and can all be subjected to the same analysis.

Some regularities appear immediately. Complexes involving pairs of rare gas atoms have minimum densities ρ_m on the order of 0.001−0.003 au, the lower values for pairs involving helium and the higher for pairs involving argon. In complexes between argon and a molecule or halide anion, ρ_m ranges from 0.003 to 0.008 au, with the larger values associated with anions or complexes in which argon participates as the base in a hydrogen bond. Complexes dominated by van der Waals forces have minimum densities in the range 0.001−0.004 au. Ion−molecule interactions have minimum densities around 0.01−0.03 au, and strongly hydrogen-bonded systems have ρ_m of ∼0.02−0.03 au. These values are consistent with Bader's observations[1] on the supermolecular electron densities at the bond critical points for van der Waals and hydrogen-bonded complexes.

Also evident are regularities in the minimum distances r_m in Table 1 (to obtain r_m relative to center B subtract the listed r_m from the listed R). For instance, the average r_m for helium is 1.40 Å, that for neon is 1.56 Å, and for argon 1.82 Å, with very little spread. For water, the minimum occurs around 1.35 Å for approach to oxygen, and at 1.79 Å along the hydrogen bond.

Note that the interactions whose geometries are derived from condensed-phase measurements are consistently longer in intermolecular distance and thus lower in minimum density than those from gas-phase complexes. The effect is especially pronounced in the alkali halides, for which the typical internuclear distance increases by 0.4−0.5 Å in going from isolated molecule to crystal, and ρ_m falls by 50 to 60%. Most other systems where comparison is possible show the same effect, but with reduced amplitude. In alkali halide crystals, this effect is due to the offsetting attractive and repulsive forces between ions. In liquid systems, such as lithium in water, molecular motions dictate that a measurement will sample a range of configurations in addition to that of lowest energy. (The exception to this trend is water, in which the cooperative effect of the hydrogen bond network in the liquid is to reduce the O—O distance relative to that in the gas-phase dimer.)

In using electron densities to describe intermolecular interactions, we need to discriminate between the van der Waals or other weakly bound systems and systems such as hydrogen-bonded or ion−molecule pairs. When strong, directional forces are involved, the densities and distances reported in Table 1 are appropriate for the geometries quoted but not representative of other orientations. The weakly bound systems, on the other hand, are much more readily described by their density minima independent of orientation. Among the weakly interacting systems, we observe that the minimum electron densities span the range from 0.001 to 0.006 au, with a peak around 0.004 au. Determining a molecular isodensity contour from this is not simply a matter of dividing by two, however. The term ρ_m is a property of the supermolecule, and its constituent molecules usually make different contributions at r_m. To discern molecular contributions, we need to use our earlier finding that supermolecular densities are essentially additive in the region of the minimum. This leads us to the model presented in the next section.

A Simple Model for Interacting Densities

The density functions described to this point are numerical; that is, they have been determined from wave functions by pointwise evaluation on a grid. There are some analytical approximations one can make that facilitate their interpretation. At sufficiently large distances from the nuclei, atomic and

TABLE 2: Exponential Fits[a] of Molecular Electron Density Functions in the van der Waals Region

molecule	direction[b]	C_M, au	α_M, Å^{-1}
He		1.542	5.505
Ne		11.82	6.052
Ar		4.530	4.243
Li^+		8.635	9.393
Na^+		20.29	7.590
F^-		1.506	3.807
Cl^-		1.033	2.978
H_2**O**	lone pair (45° from symmetry axis)	4.139	4.182
	0° from symmetry axis	3.166	4.389
	extension of OH bond	28.04	4.783
H**F**	extension of FH bond	16.08	4.794
	at F on axis	6.459	5.493
	at F ~45° from axis	8.230	5.133
CH_4	extension of CH bond	37.02	4.303
	along C_{3v} axis opposite CH bond	1.566	3.836
NH_4^+	extension of NH bond	67.54	5.162
H_2**C**=**C**H_2	out of plane, perpendicular to bond at midpoint	0.989	3.257
	in plane, perpendicular to bond at midpoint	0.939	3.500
H_2C=**C**H_2	out of plane, above C	0.871	3.235
O**C**O	perpendicular to molecular axis	2.420	4.447
OC**O**	approximately perpendicular to axis	3.368	4.517

[a] Fits were performed over a range of values of r for which $0.016 > \rho > 0.0001$ au. [b] The local origin for the coordinate r is the nucleus or bond center indicated in boldface.

molecular electron densities are essentially exponential in radial directions.[44] Distances of interest in this work are on the order of the van der Waals radii (i.e., 1.0 to 1.6 Å for most first-row atoms), at which the electron densities are generally between 0.02 and 0.0001 au. For the density in a radial direction, one can write

$$\rho_M^{\text{fit}}(r_M) = C_M \exp(-\alpha_M r_M) \tag{4}$$

and fit C_M and α_M by least squares to computed electron densities on the specified line. Here M represents a particular molecule and direction, and superscript fit denotes a fitted quantity. Clearly, eq 4 is only meaningful over the range of r in which the fit is performed. (The wave functions used here are assembled from linear combinations of primitive Gaussian functions, which of course do not individually decay exponentially. However, the Gaussian basis set is sufficiently flexible that the density function maintains single-exponential character to densities of magnitude $<10^{-5}$ au.)

The fitted supermolecular electron density along the intermolecular line is given by the sum of fitted molecular densities; that is

$$\rho_{AB}^{\text{fit}}(r;\boldsymbol{R}) = \rho_A^{\text{fit}}(r) + \rho_B^{\text{fit}}(R-r) \tag{5}$$

where R is the intermolecular distance and r lies along the line defined by the vector $\boldsymbol{R}$. This relationship suggests another difference density function, namely,

$$\Delta\rho_{AB}^{\text{fit}}(r;\boldsymbol{R}) = \rho_{AB}(r;\boldsymbol{R}) - \rho_{AB}^{\text{fit}}(r;\boldsymbol{R}) \tag{6}$$

which is only defined in directions and ranges for which density function fits have been made, but which compresses considerable information when its use is appropriate. As we already did for ρ and ρ^0, we can define a minimum distance r_m^{fit} for ρ_{AB}^{fit}. With the help of eq 4, we have

$$r_m^{\text{fit}} = (\alpha_A + \alpha_B)^{-1}\{\ln(C_A\alpha_A/C_B\alpha_B) + \alpha_B R\} \tag{7}$$

with r_m^{fit} relative to center A.

Table 2 contains exponential fits according to eq 4 for the molecular systems treated in Table 1. Because the fitting range is limited to distances for which $0.016 > \rho > 0.0001$ au, the quality of the fits is quite good, with correlation coefficients typically >0.999. Electron density minima and minimum distances determined with eqs 5 and 7 are given in Table 1 in the columns labeled $\rho^{\text{fit}}(r_m)$ and r_m^{fit}. It is evident that agreement between computed and fitted values is excellent in almost all cases. The cases of worse agreement are associated with the most strongly interacting systems. The largest difference between r_m and r_m^{fit}, 0.064 Å, occurs for gas-phase Li^+Cl^-. Most such differences are 0.02 Å or less. Likewise, the largest fractional differences between $\rho(r_m)$ and $\rho^{\text{fit}}(r_m^{\text{fit}})$, ~30%, occur in the alkali halide systems. Otherwise, these differences are <10%. In general, even in strongly hydrogen-bound systems, eqs 4−7, which are based on properties of the individual molecules, provide a quite satisfactory approximation to numerical densities and minima obtained from the supermolecule calculations.

The terms $\Delta\rho_{AB}$ and $\Delta\rho_{AB}^{\text{fit}}$ are compared graphically in Figure 3 for the systems depicted in Figures 1 and 2. The supermolecular electron densities for Na^+—OH_2 and Ne—FH are shown in Figures 3(a) and 3(c), along with the corrresponding molecular densities. The difference densities defined by eqs 2 and 6 are shown in Figures 3(b) and 3(d). The term $\Delta\rho_{AB}$ is well defined over the entire range of R, but $\Delta\rho_{AB}^{\text{fit}}$ is only defined over the range for which eq 4 is appropriate. In each case, the fitted result is of almost the same quality as the difference of numerical results in the region of the minimum. However, the fitted results lose accuracy as one moves outside the region on which they were defined.

The data in Table 1 and Figure 3 indicate that the exponential fitting of isolated molecule densities can be used to estimate the magnitudes of intermolecular minimum densities to <20% and their positions to within 0.04 Å. For cases in which typical intermolecular geometries can be estimated, this gives a very simple and inexpensive method of determining molecular size and shape in a condensed medium.

With the aid of eqs 4−7 and the parameters of Table 2, we can determine the density contributions of molecules A and B at the minimum density position of system AB. These molecular values are of greatest interest in specifying an isodensity surface that describes the size and shape of a molecule in

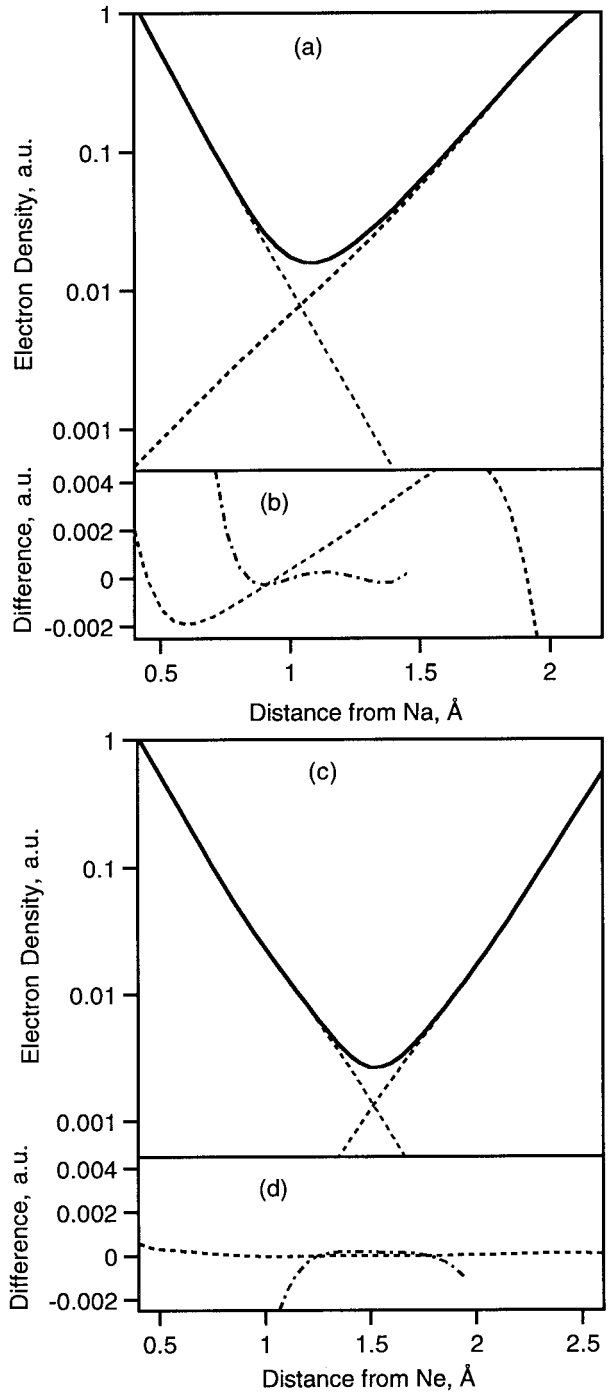

Figure 3. (a) Total electron density (solid line) for $Na^+—OH_2$ along ***R***, which runs from Na to O. Isolated molecular densities (dashed lines) for Na^+ and H_2O. (***R*** corresponds to the line joining Na and O in Figure 1.) (b) Difference between the total density and the sum of Na^+ and H_2O densities (dashed line), and between the total density and the sum of Na^+ and H_2O exponential fitted densities (chained line). (c) As (a), for the Ne—FH system; ***R*** runs from Ne to F. (d) As (b), for the Ne—FH system. Note that the linear scales in (b) and (d) cover a small range about zero.

condensed media. The results of that effort appear in Table 3. The distribution of densities is essentially bimodal: Weakly interacting systems have an average density contribution from each molecule of 0.00199 ± 0.00139 au, whereas hydrogen bonding, ion−ion and ion−dipole systems have an average density of 0.0126 ± 0.0084 au. The large standard deviations reflect the diversity of interactions in the database of Table 1.

Discussion

The additive character of intermolecular electron densities just demonstrated has previously been noted in other contexts. Gordon and Kim[45] developed a theory of forces between closed-shell atoms in which the sum of unperturbed atomic densities was used to evaluate all terms in the interaction potential. Carroll and Bader[46] applied the atoms in molecules approach to a series of bases hydrogen-bonded to hydrogen fluoride, and demonstrated that the density at the hydrogen bond critical point is well approximated by the sum of isolated molecule densities. Results given there are consistent with results in Table 1, allowing for somewhat different supermolecular geometries. Bone and Bader[47] made comparable observations for a set of twelve van der Waals complexes. The present study is akin to the work of Gordon and Kim[45] in that it provides a way to employ only the molecular electron densities to obtain information about the intermolecular complex.

In the previous section we arrived at an electron density contour of ∼0.002 au as an appropriate average value for describing the size and shape of a weakly interacting molecule in condensed media. This particular value has been arrived at by numerous other studies from different criteria. As mentioned in the *Introduction*, Bader et al.[3] suggested it on theoretical grounds. Empirical justifications were provided by its usefulness in describing the packing of O_2 or N_2 molecules in their solid phases,[48,49] and by its ability to correlate with molecular sizes inferred from gas-phase kinetic theory data.[3] However, we have shown that the relative standard deviation about this value is 70%. In addition, the same molecule may have a different size in different environments, as shown by the data in Table 3. Clearly, there is no universal size-determining contour. When no better information is at hand, the 0.002 au contour is an appropriate estimate, but more specific information, such as that in the Tables, should guide one's choice.

In the cases reported in Table 1 we have used molecular configurations that represent equilibrium geometries, except for the liquid diffraction results that represent average geometries. In a condensed medium, many nearest-neighbor pairs will be oriented relative to one another in configurations that do not resemble the equilibrium geometries used here. What effect will these variations have on the results already discussed? In systems that are dominated by van der Waals attractions, there is little directional character to the intermolecular binding, and conclusions are not expected to be much affected. We demonstrate this phenomenon in Figure 4, in which we compare semiempirical estimates of intermolecular distances with estimates derived from the present density-based method. For the systems helium—carbon dioxide, argon—carbon dioxide, and neon—hydrogen fluoride, two-dimensional potential energy surfaces have been published. The first two are based on multiproperty fits to a parametrized potential function,[18,26] the third on an ab initio calculation that reproduces experimental trends in IR spectra.[12]

The He−CO_2 density-generated estimate is based on combining the distances at which He and CO_2 each contribute 0.0008 au to the intermolecular density; that is,

$$R_{\mathrm{HeB}} = r_{\mathrm{He}}(0.0008) + r_{\mathrm{B}}(0.0008)$$

with r_{He} defined by

$$\rho_{\mathrm{He}} = 0.0008 \text{ au} = C_{\mathrm{He}} \exp[-\alpha_{\mathrm{He}} r_{\mathrm{He}}(0.0008)]$$

with a corresponding definition for r_{B}, where B is carbon or

TABLE 3: Molecular "Sizes" and Electron Densities from Interaction Distances

molecule A	interacting with	r_m^f, Å	$\rho_A(r_m)$, au	molecule A	interacting with	r_m^f, Å	$\rho_A(r_m)$, au
He	He	1.485	0.00043	Cl^-	Ne	2.26	0.00124
	Ne	1.389	0.00074		Ar	1.94	0.00322
	Ar	1.411	0.00065		H_2O	1.472	0.0129
	Na^+	1.19	0.00224		Li^+ (crystal)	1.687	0.00680
	F^-	1.48	0.00044		Li^+ (gas)	1.270	0.0235
	CO_2	1.38	0.00076		Na^+ (crystal)	1.655	0.00747
	CH_4	1.43	0.00058		Na^+ (gas)	1.325	0.0199
Ne	He	1.616	0.00067	H_2O (lone pair)	H_2O (dimer)	1.32	0.0113
	Ne	1.55	0.00100		H_2O (liquid)	1.29	0.0163
	Ar	1.577	0.00085		NH_4^+	1.38	0.0129
	F^-	1.50	0.00132		Li^+	1.44	0.00991
	Cl^-	1.63	0.00061		Na^+	1.39	0.0125
	HF (H end)	1.50	0.00138	H_2O (C_{2v})	Li^+	1.14	0.0214
	HF (F end)	1.52	0.00119		HF	1.19	0.0170
	CH_4	1.61	0.00070		CH_4	1.61	0.00483
Ar	He	2.023	0.00085		CO_2	1.43	0.00587
	Ne	1.939	0.00121	H_2O (along H)	Ar	1.88	0.00217
	Ar	1.88	0.00156		H_2O (dimer)	1.66	0.00998
	F^-	1.61	0.00486		H_2O (liquid)	1.56	0.0186
	Cl^-	1.79	0.00226		Cl^-	1.706	0.00802
	HF (bent)	1.85	0.00174		CH_4	2.01	0.00190
	HF (H end)	1.71	0.00322	HF (H end)	Ne	1.90	0.00175
	HF (F end)	1.79	0.00225		Ar	1.80	0.00285
	H_2O	1.77	0.00244		H_2O	1.45	0.0155
	CO_2	1.85	0.00175		C_2H_4	1.57	0.00594
	CH_4 (face)	1.83	0.00193		HF	1.53	0.0100
	CH_4 (along H)	1.77	0.00252	HF (F end)	Ne	1.55	0.00131
	C_2H_4	1.86	0.00173		Ar	1.50	0.00174
Li^+	H_2O (nonplanar)	0.81	0.00441		Li^+	1.076	0.0175
	H_2O (planar)	0.72	0.0100	HF (F end, bent)	Ar	1.69	0.00144
	F^- (crystal)	0.781	0.00561		HF	1.22	0.0105
	F^- (gas)	0.652	0.0190	CH_4 (along H)	Ar	2.23	0.00248
	Cl^- (crystal)	0.883	0.00216		H_2O	2.09	0.00470
	Cl^- (gas)	0.751	0.00746		CH_4	2.29	0.00196
	HF (F end)	0.717	0.0103	CH_4 (C_{3v})	He	1.97	0.00083
	C_2H_4	0.862	0.00263		Ne	1.89	0.00111
Na^+	He	1.24	0.00162		Ar	1.72	0.00213
	H_2O (nonplanar)	1.05	0.00689		H_2O	1.69	0.00237
	F^- (crystal)	1.063	0.00637		CH_4	1.71	0.00220
	F^- (gas)	0.944	0.0157	NH_4^+ (along H)	H_2O	1.70	0.0104
	Cl^- (crystal)	1.165	0.00293	C_2H_4 (in plane)	Ar	1.74	0.00209
	Cl^- (gas)	1.036	0.00783	C_2H_4 (out of plane)	Li^+	1.496	0.00757
F^-	He	2.04	0.00064		HF	1.73	0.00403
	Ne	1.73	0.00210	C_2H_4 (carbon to carbon)	C_2H_4	1.98	0.00146
	Ar	1.48	0.00541	CO_2 (perpendicular from C)	He	1.77	0.00094
	Li^+ (crystal)	1.232	0.0138		Ar	1.64	0.00167
	Li^+ (gas)	0.912	0.0467		H_2O	1.36	0.00580
	Na^+ (crystal)	1.254	0.0127				
	Na^+ (gas)	1.018	0.0312				

oxygen depending on the direction of approach. The choice of density contour value is guided by ρ_m in Table 1. It can be seen that the size and shape so derived conform well to the semiempirical surface, the major discrepancy coming at the linear O−C−O−He configuration. This discrepancy may not be entirely the fault of the density method. The linear configuration is a saddle point on the potential surface and not well characterized by the experimental data; the parameters in the potential that describe it are assigned fixed values. The Ar−CO_2 density-generated estimate is based on 0.002 au contributions to the intermolecular density. Table 1 would have suggested a value of ∼0.0017 au, close enough to the recommended average value of 0.002 that the differences are slight. The same general trends are observed as for He−CO_2, and the same caveat about the linear structure applies. The Ne−HF estimates use a density of 0.0012 au, with quite satisfactory agreement with the ab initio surface. Using a density value of 0.002 au would have resulted in decreases of ∼0.18 Å in all the intermolecular distances, which is still in reasonable agreement with the surface of O'Neil et al.[12]

Strongly interacting systems are highly directional, and reorientation of the molecules leads to considerable variation of interaction energies and distances. For instance, the geometry and energetics of the hydrogen fluoride dimer are dominated by the dipole−dipole interaction term. Any configuration that allows a hydrogen to approach a fluorine will generate substantial attraction, with the short distances and large minimum electron densities already described. On the other hand, any configuration that forces both fluorines or both hydrogens together will be so repulsive that the molecules cannot approach close enough to have significant ($>10^{-6}$ au) density overlap. In some intermediate orientations, for instance, that of an elongated tetrahedron, the dipole−dipole term is minimized and the distances and densities will be typical of weaker interactions.

Due to this variability when strong, directional forces are present, the current method of analyzing the interaction between one molecule and another does not give us enough information about the interaction between a particular molecule and all its nearest neighbors in condensed phases. However, if a configuration involving a molecule and a set of its neighbors is

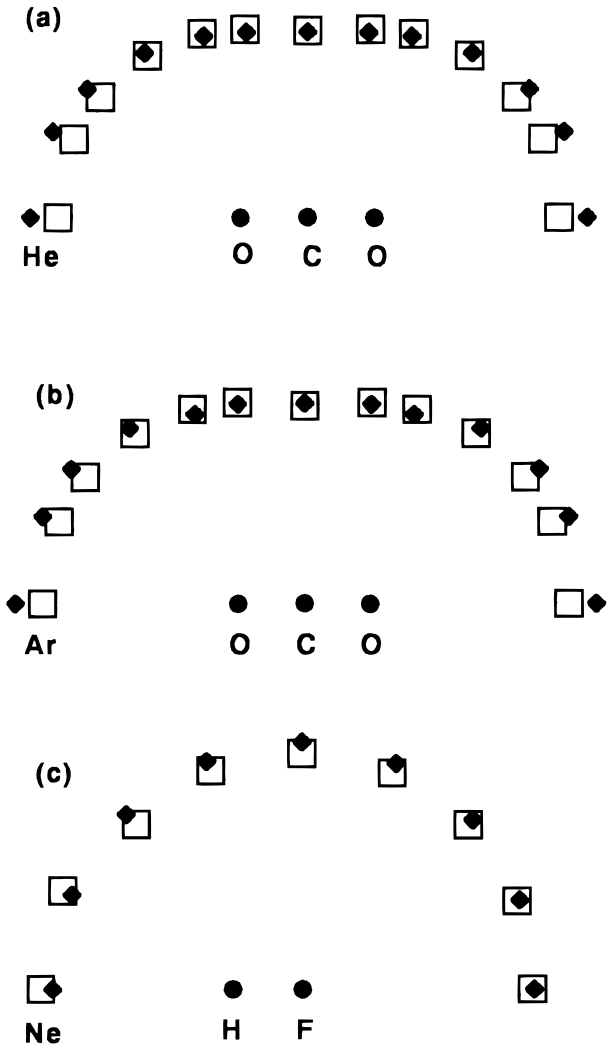

Figure 4. (a) Position of potential surface minimum as a function of angle for helium interacting with carbon dioxide. Solid diamonds represent the semiempirical surface of Beneventi et al.,[18] and open squares represent the estimate of the density model as described in the text. (b) As (a) for the argon—carbon dioxide surface of Bohac et al.[26] (c) As (a) for the neon—hydrogen fluoride surface of O'Neil et al.[12]

available, for instance, from a molecular dynamics simulation or an X-ray diffraction structure, the current method including exponential fitting can readily be applied to specify the size and shape of the molecule in that particular environment.

Recent work by Wiener et al.[50,51] has indicated that the minimum in the electrostatic potential along a line between neighboring nuclei provides a good definition of covalent radii. We briefly explored the possibility of applying this criterion for intermolecular interactions, but found it of no use in the present context. The reason is quite simple: Around electropositive atoms, the potential remains positive as one moves away from the nucleus. Around electronegative atoms, the potential eventually goes negative. The total potential along the line joining atoms in different molecules is essentially the sum of the isolated molecular potentials. When an electropositive atom interacts with an electronegative atom, the minimum is always displaced toward the electronegative atom. For instance, in the HeF^- system, the potential of strongly electronegative fluoride overwhelms that of weakly electropositive helium and the minimum in the electrostatic potential occurs 2.45 Å from the helium nucleus, compared with 1.48 Å for the density minimum.

Possible Application to Dielectric Continuum Models of Solvation

Some of the interest in electron density contours as descriptors of molecular size and shape arises from their recent incorporation in quantum chemistry suites[7,9] as parameters in dielectric continuum calculations of molecular solvation. From the earliest days of dielectric continuum models of solvation,[52] specification of the size of the cavity that contains the solute molecule has been rather arbitrary. In the absence of an a priori way to establish cavity dimensions, considerable experimentation has been done with spheres and ellipsoids, atomic van der Waals radii, group radii, and empirical scale factors.[53] The use of electron density isocontours to define cavity boundaries reduces the variability to a single quantity, the chosen electron density contour value. Wong et al.[6] specified a value of 0.001 au because it had been suggested by Bader et al.[54] as best describing molecular dimensions in the gas phase. Zhan et al.[7] employed the same value for purposes of comparison. Wiberg et al.[55] prefer a value of 0.0004 au as being better able to reproduce experimental liquid molar volumes.

What bearing do the present results have on the size and shape of a solute cavity in a liquid environment? The cavity defines the extent of a molecule by its ability to exclude its solvent neighbors from a particular region of space. A definition based on electron density minima is democratic, that is, it provides the same treatment to all molecules involved in the interacting system. A definition in terms of atomic van der Waals radii of solute and solvent would be similarly democratic. On the other hand, all continuum dielectric models are undemocratic; that is, they treat the solute molecule in a fundamentally different way from the solvent molecules. In implementations based on van der Waals radii, it has been reported[56,57] that the best agreement between calculated and experimental free energies of hydration arises when the cavity shape is obtained using atomic spheres ~20% larger than the van der Waals radii. This puts the solute cavity boundary a small distance within the solvent molecule, as defined by the solvent's van der Waals radius. The asymmetry between solvent and solute can be rationalized by pointing out that the dielectric continuum boundary is the locus for the response of the solvent to the solute; the interior of the solvent molecule makes a greater contribution to that response than does the periphery.

It was just shown that the contour value at the density minimum varies systematically with the nature of the intermolecular interaction. When this observation is applied to the potential application of defining molecular cavities in dielectric continua, the most important range is that of the weaker interactions because the dielectric continuum models of solvation are most suitable for nonspecific electrostatic interactions. Based on the results already discussed, a cavity-defining contour of 0.002 au seems an appropriate upper limit for neutral solutes with poor hydrogen-bonding prospects. Because of the inherent asymmetry between solute and solvent in dielectric continuum models, the appropriate contour for use in such models should not be larger than that determined by the present procedure. Such a specification should be well tested before being applied for general use. Appropriate tests are under way in this laboratory.[58]

Conclusion

We have used the minima in intermolecular electron densities based on experimentally and theoretically determined interaction geometries to identify an isodensity contour with the least mutual penetration of electron densities of interacting molecules. In

situations in which strong, directional interactions (e.g., hydrogen bonds or nearby ions) are absent, we have found, in agreement with others, that the 0.002 au isodensity contour is appropriate for identifying molecular approach distances in the condensed phase. When strong forces are present, a contour in the range of 0.01 to 0.02 au is more appropriate, but only at the sites and in the directions in which the force operates. Thus, no ready generalization is offered for such systems; more must be known about the nearest neighbor positions and orientations to characterize their sizes and shapes.

Acknowledgment. Valuable discussions with Dr. D. M. Chipman are gratefully acknowledged. The research described herein was supported by the Office of Basic Energy Sciences of the U.S. Department of Energy. This is contribution no. NDRL-4058 from the Notre Dame Radiation Laboratory.

References and Notes

(1) Bader, R. F. W. *Atoms in Molecules. A Quantum Theory*; Clarendon: Oxford, 1994.
(2) Stewart, R. F. In *Critical Evaluation of Chemical and Physical Structural Information*; Lide, J. D. A.; Paul, M. A., Eds.; National Academy of Sciences: Washington, D. C., 1974; p 540.
(3) Bader, R. F. W.; Henneker, W. H.; Cade, P. E. *J. Chem. Phys.* **1967**, *46*, 3341.
(4) Kihara, T.; Sakai, K. *Acta Crystallogr. A* **1978**, *34*, 326−329.
(5) Lim, C.; Chan, S. L.; Tole, P. In *Structure and Reactivity in Aqueous Solution. Characterization of Chemical and Biological Systems*; American Chemical Society: Washington, D. C., 1994; pp 50−59.
(6) Wong, M. W.; Wiberg, K. B.; Frisch, M. J. *J. Comput. Chem.* **1995**, *16*, 385−394.
(7) Zhan, C.-G.; Bentley, J.; Chipman, D. M. *J. Chem. Phys.* **1998**, *108*, 177.
(8) Gourary, B. S.; Adrian, F. J. In *Solid State Physics. Advances in Research and Applications*; Seitz, F.; Turnbull, D.; Ed.; Academic: New York, 1960; Vol. 10; p 128.
(9) Frisch, M. J.; Trucks, G. W.; Schlegel, H. B.; Gill, P. M. W.; Johnson, B. G.; Robb, M. A.; Cheeseman, J. R.; Keith, T.; Petersson, G. A.; Montgomery, J. A.; Raghavachari, K.; Al-Laham, M. A.; Zakrzewski, V. G.; Ortiz, J. V.; Foresman, J. B.; Peng, C. Y.; Ayala, P. Y.; Chen, W.; Wong, M. W.; Andres, J. L.; Replogle, E. S.; Gomperts, R.; Martin, R. L.; Fox, D. J.; Binkley, J. S.; Defrees, D. J.; Baker, J.; Stewart, J. P.; Head-Gordon, M.; Gonzalez, C.; Pople, J. A. *Gaussian 94*, Revision B.3; Gaussian, Inc.: Pittsburgh, PA, 1995.
(10) Wiberg, K. B.; Hadad, C. M.; LePage, T. J.; Breneman, C. M.; Frisch, M. J. *J. Phys. Chem.* **1992**, *96*, 671.
(11) Caminiti, R.; Licheri, G.; Paschina, G.; Pinna, G. *J. Chem. Phys.* **1981**, *72*, 4552.
(12) O'Neil, S. V.; Nesbitt, D. J.; Rosmus, P.; Werner, H.-J.; Clary, D. C. *J. Chem. Phys.* **1989**, *91*, 711.
(13) Boys, S. F.; Bernardi, F. *Mol. Phys.* **1970**, *19*, 553.
(14) Burgmans, A. J. L.; Farrar, J. M.; Lee, Y. T. *J. Chem. Phys.* **1976**, *64*, 1345.
(15) Maitland, C. E.; Wakeham, W. A. *Mol. Phys.* **1978**, *35*, 1443.
(16) Moszynski, R.; Wormer, P. E. S.; Viehland, L. A. *J. Phys. B: At. Mol. Opt. Phys.* **1994**, *27*, 4933.
(17) Moszynski, R.; Jeziorski, B.; Szalewicz, K. *Chem. Phys.* **1992**, *166*, 329.
(18) Beneventi, L.; Casavecchia, P.; Vecchiocattivi, F.; Volpi, G. G.; Buck, U.; Lauenstein, C.; Schinke, R. *J. Chem. Phys.* **1988**, *89*, 4671.
(19) Gao, D.; Chen, L.; Li, Z.; Tao, F.-M.; Pan, Y.-K. *Chem. Phys. Lett.* **1997**, *277*, 483.
(20) Farrar, J. M.; Lee, Y. T.; Goldman, W.; Klein, M. L. *Chem. Phys. Lett.* **1973**, *19*, 359.
(21) Kellö, V.; Sadlej, A. J. *Chem. Phys.* **1991**, *157*, 123.
(22) Colbourn, E. A.; Douglas, A. E. *J. Chem. Phys.* **1976**, *65*, 1741.
(23) Harris, S. J.; Novick, S. E.; Klemperer, W. *J. Chem. Phys.* **1974**, *60*, 3208.
(24) Hutson, J. M. *J. Chem. Phys.* **1992**, *96*, 6752.
(25) Cohen, R. C.; Saykally, R. J. *J. Chem. Phys.* **1993**, *98*, 6007.
(26) Bohac, E. J.; Marshall, M. D.; Miller, R. E. *J. Chem. Phys.* **1992**, *97*, 4890.
(27) Buck, U.; Kohlhase, A.; Phillips, T.; Secrest, D. *Chem. Phys. Lett.* **1983**, *98*, 199.
(28) Liu, W. L.; Kolenbrander, K. L.; Lisy, J. M. *Chem. Phys. Lett.* **1984**, *112*, 585.
(29) Dyke, T. R.; Mack, K. M.; Muenter, J. S. *J. Chem. Phys.* **1977**, *66*, 498.
(30) Narten, A. H.; Levy, H. A. *J. Chem. Phys.* **1971**, *55*, 2263.
(31) Narten, A. H.; Vaslow, F.; Levy, H. A. *J. Chem. Phys.* **1973**, *58*, 5017.
(32) Pálinkás, G.; Radnai, T.; Szász, G. I.; Heinzinger, K. *J. Chem. Phys.* **1981**, *74*, 3522.
(33) Del Bene, J. E.; Frisch, M. J.; Raghavachari, K.; Pople, J. A.; Schleyer, P. v. R. *J. Phys. Chem.* **1983**, *87*, 73.
(34) Kollman, P.; McKelvey, J.; Johansson, A.; Rothenberg, S. *J. Am. Chem. Soc.* **1975**, *97*, 955.
(35) Dore, L.; Cohen, R. C.; Schmuttenmaer, C. A.; Busarov, K. L.; Elrod, M. J.; Loeser, J. G.; Saykally, R. J. *J. Chem. Phys.* **1994**, *100*, 863.
(36) Block, P. A.; Marshall, M. D.; Pedersen, L. G.; Miller, R. E. *J. Chem. Phys.* **1992**, *96*, 7321.
(37) Habenschuss, A.; Johnson, E.; Narten, A. H. *J. Chem. Phys.* **1981**, *74*, 5234.
(38) van Nes, G. J. H.; Vos, A. *Acta Crystallogr.* **1979**, *B35*, 2593.
(39) Barton, A. E.; Chablo, A.; Howard, B. J. *Chem. Phys. Lett.* **1979**, *60*, 414.
(40) Brigot, N.; Odiot, S.; Walmsley, S. H.; Whitten, J. L. *Chem. Phys. Lett.* **1977**, *49*, 157.
(41) Bunker, P. R.; Jensen, P.; Karpfen, A.; Kofranek, M.; Lischka, H. *J. Chem. Phys.* **1990**, *92*, 7432.
(42) Donnay, J. D. H.; Donnay, G.; Cox, E. G.; Kennard, O.; King, M. V. *Crystal Data, Determinative Tables*, 2nd ed.; American Crystallographic Assn.: Pittsburgh, PA, 1963.
(43) Huber, K. P.; Herzberg, G. *Molecular Spectra and Molecular Structure. Vol. 4: Constants of Diatomic Molecules*; Van Nostrand Reinhold: New York, 1979.
(44) Ahlrichs, R. *Chem. Phys. Lett.* **1972**, *15*, 609.
(45) Gordon, R. G.; Kim, Y. S. *J. Chem. Phys.* **1972**, *56*, 3122−3133.
(46) Carroll, M. T.; Bader, R. F. W. *Mol. Phys.* **1988**, *65*, 695−722.
(47) Bone, R. G. A.; Bader, R. F. W. *J. Phys. Chem.* **1996**, *100*, 10892−10911.
(48) Barrett, C. S.; Meyer, L.; Wasserman, J. *J. Chem. Phys.* **1967**, *47*, 595.
(49) Schuch, A. F.; Mills, R. L. *J. Chem. Phys.* **1970**, *52*, 6000.
(50) Wiener, J. J. M.; Grice, M. E.; Murray, J. S.; Politzer, P. *J. Chem. Phys.* **1996**, *104*, 5109−5111.
(51) Wiener, J. J. M.; Murray, J. S.; Grice, M. E.; Politzer, P. *Mol. Phys.* **1997**, *90*, 425−430.
(52) Born, M. *Z. Phys.* **1920**, *1*, 45.
(53) Tomasi, J.; Persico, M. *Chem. Rev.* **1994**, *94*, 2027−2094.
(54) Bader, R. F. W.; Carroll, M. T.; Cheeseman, J. R.; Chang, C. *J. Am. Chem. Soc.* **1987**, *109*, 7968−7979.
(55) Wiberg, K. B.; Keith, T. A.; Frisch, M. J.; Murcko, M. *J. Phys. Chem.* **1995**, *99*, 9072−9079.
(56) Miertus, S.; Scrocco, E.; Tomasi, J. *Chem. Phys.* **1981**, *55*, 117−129.
(57) Luque, F. J.; Negre, M. J.; Orozco, M. *J. Phys. Chem.* **1993**, *97*, 4386−4391.
(58) Zhan, C.-G.; Chipman, D. M., submitted for publication.